Broadening the Specification of Granular Fills

M. D. BOLTON, R. J. FRAGASZY, AND D. M. LEE

Triaxial tests have been carried out on unconventional fills. The shear strengths of gap-graded fills, with 15 and 30 percent of large particles in a fine matrix of sand, were compared with the matrix alone at a range of relative densities. It was found that when present at 30 percent, the large particles provide additional strength, whereas at 15 percent, they have an adverse effect. Possible mechanisms for these phenomena are discussed. Strength enhancement was still available when the large particles were of poor quality, friable limestone. These laboratory trials suggest that a more flexible specification for fill could lead to significant economies, but further tests will be required for confirmation.

In the United Kingdom, materials for use as backfill to retaining structures and as general fill are specified in the *Specification for Highway Works*, which was compiled by the Department of Transport in 1986 (*1*). This serves mainly as a guide for structures of moderate size (less than 15 m), typical of the requirements for road embankments. The specification allows particle sizes up to 75 mm to be used behind retaining structures (Figure 1) and up to 500 mm for general fills. It is apparent that the physical dimension of these large particles poses some difficulties in laboratory testing, which will be discussed in this paper.

Granular soils comprising sound particles with sizes distributed on smooth grading curves and a high uniformity coefficient (C_u) have generally been employed as backfill. A uniformity coefficient of 5 is thought to be the minimum required to obtain high dry density under mechanical compaction. Particle soundness is generally assessed by the 10 percent fines method (BS812 1975, Part 3, Method 8), which measures the load in static compaction on a sample of circa 10-mm-diameter particles, such that 10 percent by weight of particles finer than 2.4 mm are produced.

In the wider context of ascribing material parameters to soils containing large particles, it is of interest to explore whether their specification can be broadened to include certain granular fills that would be regarded as unconventional. Unconventional fills can be placed in two categories. The first contains fills with unconventional size distributions, for example, a fill with either a discontinuous gradation or an excessive proportion of fine particles. Granular soils obtained from breaking down rock masses frequently give rise to a gap-graded size distribution, containing a small portion of much larger pieces. These pieces may be left out or subjected to additional crushing. Furthermore, in areas undergoing redevelopment, cheap granular materials are always in abundance in the form of slag, broken brick, or concrete. In such a case, it is possible to introduce these materials, in a controlled quantity, into imported high quality sand. In view of the environmental benefits of avoiding dumps and restricting new quarries, and for economic reasons, the inclusion of these waste materials is an option that should be explored. The second category contains materials that are prone to brittle fracture under moderate stress levels or when being compacted or sheared.

The angle friction, ϕ'_{crit}, for soil shearing at constant volume (in a critical state), has been found to be approximately invariable with density and stress level for a particular soil aggregate. Peak angles of shearing resistance ($\phi'_{max} > \phi'_{crit}$) are associated with dilatancy and depend on initial density and a moderate stress level. The stress (p'_{crit}) necessary to eliminate dilatancy and thereby force soil to contract toward its critical state apparently depends on its initial relative density (I_D) (*2*).

The reduction of ϕ'_{max} toward ϕ'_{crit} as a result of grain crushing has limited the use of such low-grade granular fill as weakly cemented calcareous limestone and chalk, even in small soil structures. A rare example was the use of soft reef limestone used in the Evretou Dam in Cyprus (*3*). However, if crushable materials are present in a controlled quantity within a sound material, the mixture may at least be as strong as the sound material alone at the same relative density.

GRAIN FRACTURE

A particle fragmentation test (PFT) was used to give the fracture strength of individual particles over a range of size. An Instron loading frame was used to provide a uniaxial force to crush each particle separately between two smooth platens. The diameter (d) of a particle was taken as the mean of the longitudinal and lateral dimensions. Particles with an aspect ratio close to 1 were chosen and soaked for 24 hr. In the test, the first major drop in the applied load usually signifies the first fracture along the axial direction, which can also be detected visually.

The fracture force depends on the size of the particles and their strength. The relationship can be represented after the Brazilian test for the tensile strength of concrete, by

$$P_f \propto \sigma_f \cdot d^2 \tag{1}$$

where P_f is the fracture force and σ_f is the tensile strength of the material.

Figure 2 shows that P_f/d^2 and d can be related by linear

M.D. Bolton and D.M. Lee, Department of Engineering, University of Cambridge, Trumpington Street, Cambridge. CB2 1PZ England. R.J. Fragaszy, GeoSyntec Consultants, Norcross, Ga. 30093.
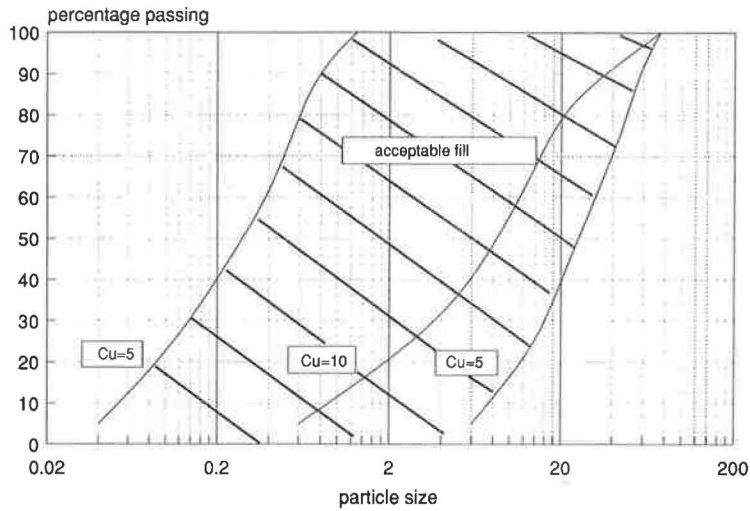
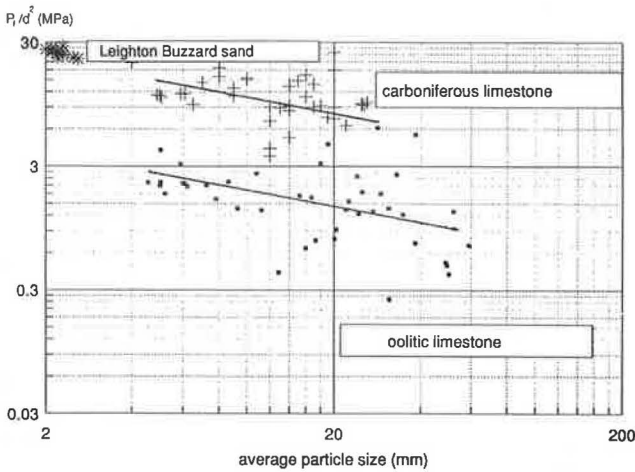FIGURE 1 Acceptable fills for structures.

FIGURE 2 Particle strength.

regression lines on logarithmic scales. An empirical relationship can be written as follows:

$$\frac{P_f}{d^2} = K \cdot d^b \tag{2}$$

where K is a material constant and b represents the slope of the plot, which is negative.

This leads to the following equation:

$$\sigma_f \propto d^b \tag{3}$$

This equation implies that a material with a slope of zero on the logarithmic plot ($b = 0$) will be "perfect" material, for which strength does not deteriorate with particle size. Brittle materials such as soil usually have a negative value of b. As a result of crack propagation from internal flaws, if the flaw size is proportional to the particle size, Griffith (4) implies the following:

$$\sigma_f \propto d^{-0.5} \tag{4}$$

A number of materials had been tested, and three were chosen for this study—Leighton Buzzard sand, oolitic limestone, and carboniferous limestone (Figure 2). The limestones gave $b \approx -0.3$.

MATERIAL PROPERTIES

The regression lines in Figure 2 show that Leighton Buzzard sand has a similar fracture strength tendency to the carboniferous limestone, whereas the oolitic limestone is approximately 5 times weaker, size by size. Large carboniferous limestone particles could therefore be treated as sound inclusions in a maxtix of sound Leighton Buzzard sand, whereas oolitic limestone inclusions can be treated as friable and low grade.

Grain properties of the three materials are presented in Table 1. The values for roundness and sphericity were assigned according to tables constructed by Krumbein (5) and Rittenhouse (6), respectively.

MATERIAL GRADATION

This gradation of samples for the triaxial tests was chosen under two conditions. The first condition concerns the maximum particle size to be included. A minimum value of 10 for the ratio (r) of sample diameter to particle size was recommended by Bishop and Henkel (7). However, lower values, such as 6 and 4, had been used by other researchers [Siddiqi (8), Marachi et al. (9), al-Hussaini (10), and Su (11)].

TABLE 1 GRAIN PROPERTIES OF MATERIALS

	Leighton Buzzard sand	oolitic limestone	carboniferous limestone
specific gravity	2.664	2.710	2.729
gradation mm	0.1-2	3.35-5.6	3.35-5.6
surface texture	smooth	very rough	rough
sphericity	0.87	0.75	0.69
roundness	0.6	0.4	0.3

It can be concluded that as the value of *r* becomes smaller than six, the strength and stiffness are somewhat enhanced as possible ruptures are impeded. In this study, the maximum particle size used was 5.6-mm in 70-mm-diameter triaxial samples. In addition, it was decided to simulate a gap-graded soil mixture. The Leighton Buzzard sand was chosen as the sound matrix material with sizes from 0.1 to approximately 2 mm. Both limestones were used as the large content with sizes from 3.35 to approximately 5.6 mm. Fills *A* and *B* contained the matrix with 15 percent by weight of oolitic and carboniferous limestones, respectively, and Fills *C* and *D* contained the matrix with 30 percent of oolitic and carboniferous limestone particles (Figure 3). In this way, the strength characteristic of the mixtures can be compared with that of the matrix alone.

TRIAXIAL TESTS

The triaxial apparatus used in Cambridge was first assembled by Houlsby (*12*). Various modifications have been made since. The current set-up consists of a Geonor cell unit with a rotating bush that reduces the ram friction. The cell pressure is provided by a mercury pot system capable of providing 650 kPa. A GDS pressure controller is used to provide the back pressure for the drained tests, as well as for measuring the volume change of the sample. The test progress is computer controlled, and measurements of axial load, volume change, and axial strain are logged and stored in disk files for post processing. The magnitudes of cell pressure and pore pressure are also monitored in all tests.

All samples were 70 mm in diameter. Greased rubber discs were used to minimize the end friction imposed by the platens. As a result of using fee ends, "dead-ends" are effectively eliminated, and samples of aspect ratio 1 can be used. All tests conducted here were drained with fully saturated samples, achieved by first flushing carbon dioxide through the sample before introducing de-aired water under a small pressure head. Skempton's parameter *B* was checked in all samples to demonstrate a value of at least 0.95.

All tests were conducted with a cell pressure of 60 kPa. Each material was tested over a range of relative density in order to establish a correlation between ϕ'_{max} and I_D. The test
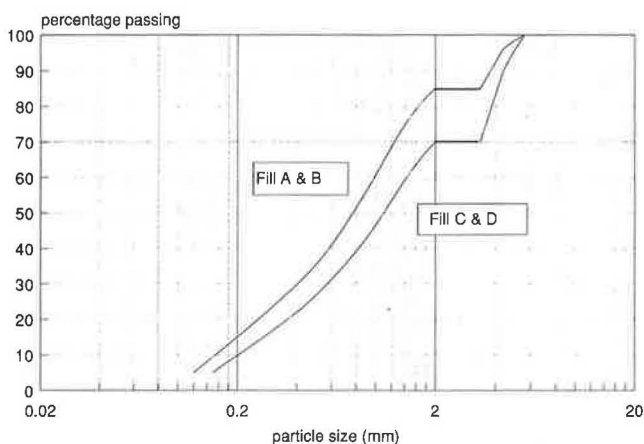
program and part of the results are presented in Table 2. Typical plots of mobilized ϕ' versus axial strain (ε_1) and volumetric strain (ε_v) versus ε_1 are shown in Figures 4 and 5.

DENSITY CORRECTION METHOD

Fragaszy et al. (*13*) discussed the behavior of sound granular fills containing various proportions of large, well-rounded, smooth particles. It was found, for smaller proportions in which the large particles could be considered to be "floating" in a finer matrix, that the strength of the total soil could be estimated as that pertaining to the matrix material remote from the large particles, discounting the looser matrix material in the zone of disturbance around each large particle. The objective of that study was to permit the modeling of the total soil aggregate by deducing an appropriate density in which to test a scalped sample of matrix material after the larger particles were removed. Because the objective here is simply to report on certain parameters affecting the strength of the total soil, no equivalent modeling criteria will be introduced to deal with these more complex materials. If the present results are considered promising, further work on the modeling of field compaction would prove desirable. Tests on fills with genuinely large particles, even maximum density tests, are difficult to achieve and validate.

TEST RESULTS

For compacted fills, the mobilized peak strength ϕ'_{max} is always used for stability or earth pressure calculations. In Figures 6

FIGURE 3 Tested unconventional fills

TABLE 2   SUMMARY OF TEST PROGRAM AND RESULTS

Test	Consolidated			ϕ'_{max} (deg)	ϕ'_{crit} (deg)
	ρ_{dry}	$v = 1 + e$	I_D		
matrix: ρ_{max} = 1.931 ρ_{min} = 1.660					
M15	1.740	1.531	32.8	38.80	38.4
M40	1.802	1.478	56.2	40.63	39.9
MM40	1.818	1.465	61.9	41.19	38.4
M60	1.882	1.410	84.1	43.16	38.6
M80	1.910	1.395	93.3	44.03	38.5
Fill A 15% oolitic limestone: ρ_{max} = 1.976 ρ_{min} = 1.670					
O15	1.824	1.464	54.5	39.31	37.4
O40	1.867	1.431	68.1	40.59	37.5
O50	1.901	1.405	78.1	42.05	*
O60	1.931	1.383	87.3	43.27	38.6
Fill B - 15% carboniferous limestone: ρ_{max} = 2.017 ρ_{min} = 1.740					
C20	1.835	1.457	37.7	39.05	38.5
C30	1.891	1.414	58.1	41.00	*
C40	1.935	1.382	73.4	42.26	38.1
C60	1.959	1.365	81.4	43.85	38.2
Fill C - 30% oolitic limestone: ρ_{max} = 2.014 ρ_{min} = 1.710					
O40-p30	1.860	1.440	53.4	41.78	40.20
O80-P30	1.931	1.387	75.8	45.46	41.30
Fill D - 30% carboniferous: ρ_{max} = 2.091 ρ_{min} = 1.800					
C40-P30	1.968	1.364	61.3	42.60	40.21
C80-P30	2.010	1.335	75.1	45.56	40.87

FIGURE 4 Axial strain versus mobilized strength (*top*) and volumetric strain (*bottom*) for Fill *A*.
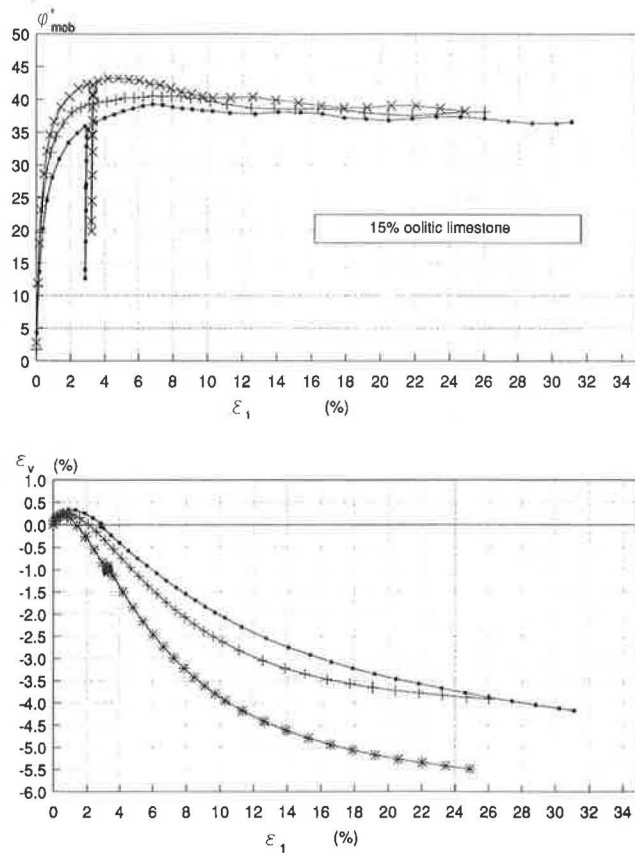

FIGURE 5 Axial strain versus mobilized strength (*top*) and volumetric strain (*bottom*) for matrix.

and 7, values of ϕ'_{max} are plotted against the relative density of the corresponding soil mixture. For this purpose, the maximum and minimum dry densities were determined following ASTM methods. The data for the matrix are plotted as a bilinear line and are treated as a norm, against which to compare other data.

It is found from the plots that ϕ'_{max} varies approximately linearly with the relative density (I_D) for each material, at least when values I_D are greater than 50 percent. When the large particle content is at 15 percent, it is observed that the rates of increase of ϕ'_{max}, with respect to I_D for the matrix, for fills A and B are all similar. However, when the large particle content is at 30 percent, the rates of increase of ϕ'_{max} for fills C and D are much higher than for the matrix.

However, perhaps more significantly, it is observed that the absolute values of ϕ'_{max} for the fills with respect to those of the matrix do not follow the same trend when the proportion of large particles is different. For fills C and D, it is found that, for values of I_D greater than 50 percent, their strengths are always higher than those of the matrix alone at the same relative density ($\sim +3°$ at $I_D = 70$ percent). It is believed that the large particles, when present in a significant quantity, act as discrete tensile reinforcing elements. This self-reinforcing effect is analogous to the enhancement of strength of triaxial samples due to rough platens.

When the amount of large particles is reduced, as in fills A and B, it might be anticipated that the reinforcing effect
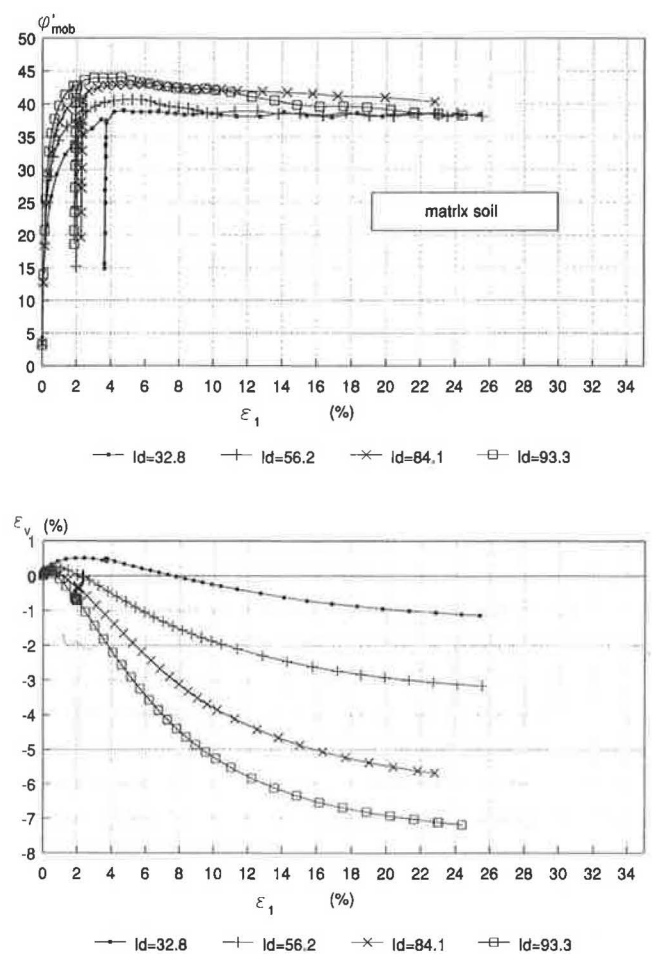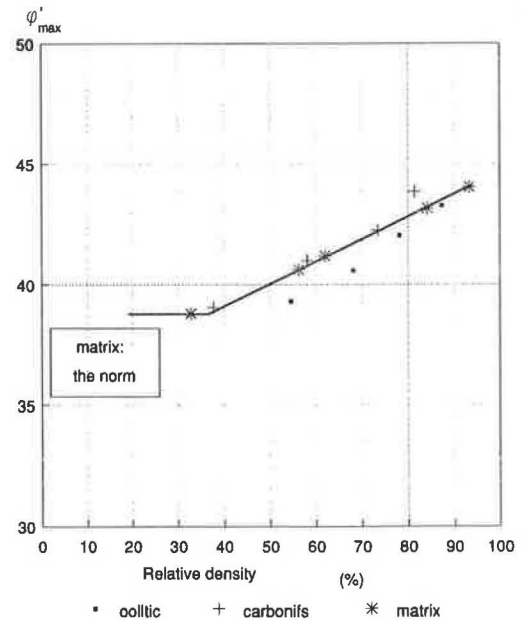

FIGURE 6 Strength versus relative density for fills *A* and *B*.

FIGURE 7   Strength versus relative density for fills *C* and *D*.

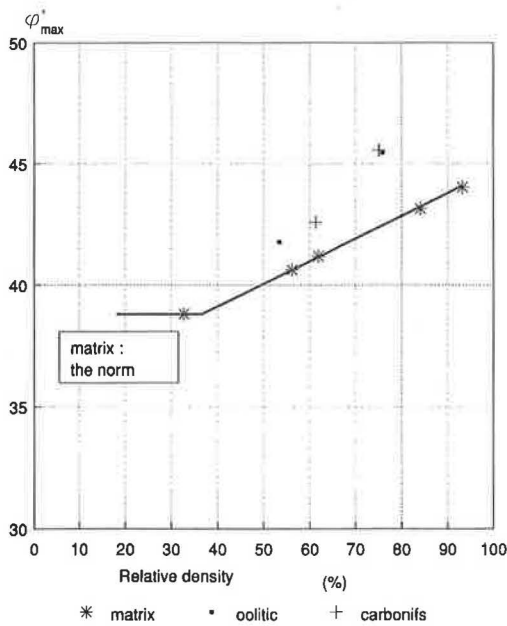FIGURE 8   Comparison of strength at 70 percent relative density.

will diminish fairly rapidly as particles are further away from each other on average, leaving the strength equal to that of the matrix. Figure 6 actually shows that for Fill *A*, which contains 15 percent of oolitic limestone in the matrix, the strength falls approximately 2° below that of the corresponding matrix at a corresponding relative density. However, this deviation might be explicable in terms of the loss of sliding resistance on or over the surfaces of occasional large particles. Each surface facet might be regarded either as inherently smoother than the matrix ($\delta < \phi'$), or as providing a zone of disturbed packing that reduces ϕ' in the near field of the matrix. It is believed that as the peak strength approaches, a rupture surface could develop in such an orientation as to entrain as many large particle facets as possible while avoiding significant intersections through the particle bodies and maintaining an angle of approximately $45 - \phi'_{max}/2$ to the major principal stress direction. The variation in relative strength is summarized in Figure 8, where $\Delta\phi'$ represents the strength of a fill in excess of that of the matrix at $I_D = 70$ percent.

In the following two sections, attempts are made to investigate the possible magnitudes of strengthening and weakening mechanisms arising from these two hypotheses.

THE DISTURBANCE MECHANISM

The situation is idealized in Figure 9 by considering a single, large cubic particle of Side *D* enclosed in a cubic cell of Side *L*, which contains a matrix of smaller particles. The volumetric proportion of large particles is:

$$R = P/(1 + e) \qquad (5)$$

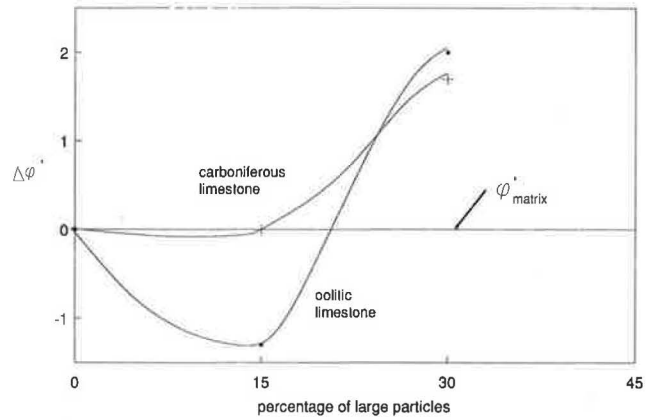where *P* is the mass proportion of cubic particles and *e* is the overall void ratio.
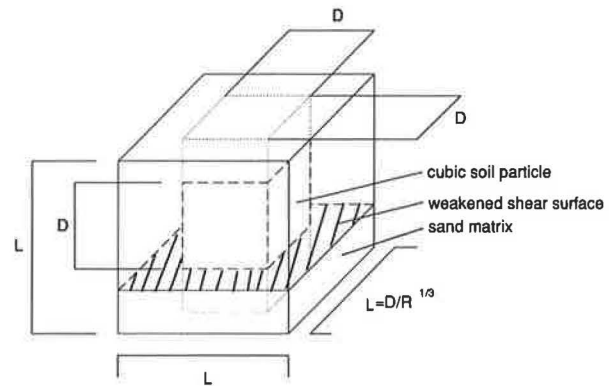

FIGURE 9   Unit cell for the disturbance mechanism model.

Then the volume of the cell is

$$L^3 = D^3/R \qquad (6)$$

The proportional area of a possible shear passing through the plane face of the particle is

$$A_R = D^2/L^2 = R^{2/3} \qquad (7)$$

Taking ϕ' in the matrix and reduced ϕ'_s on the surface of the cube, the operational strength of the weakened shear surface could be written

$$\phi'_r = A_R\phi'_s + (1 - A_R)\phi' \qquad (8)$$

This must represent the largest possible strength reduction, because it refers to coplaner particle facets.

If $\phi' = 45°$ and $\phi'_s = 30°$, then for $R = 0.15$, $A_R = 0.28$ so that $\phi'_r = 40.8°$ ($\Delta\phi' = 4.2°$). It is assumed that a rupture surface could avoid intersecting particles while passing close to the surfaces of a representative proportion of them. This calculated reduction exceeds that inferred in Figure 8 by a factor of perhaps 3. This might be taken to reflect the statistical nature of the real soil inclusions, with their random po-

sitioning. A higher proportion of large inclusions would certainly make it impossible for any such slip surface to exist.

THE REINFORCEMENT MECHANISM

Figure 10 shows a different view of the unit cell shown earlier in Figure 9, in which it is clarified that a zone of soil $D \times D \times H$ is considered to be trapped between opposing faces of large particles, considered here to be cubes in a regular array. For this sub-cell, the strength enhancement would be similar to that of soil tested in a triaxial compression between rough platens.

The following equation is derived from Equation 6:

$$H = L - D = D(1/R^{1/3} - 1) \qquad (9)$$

Figure 11 shows, in a central cross section, the equilibrium of the central zone of matrix material. The magnitude of end friction can be taken to be $\mu\sigma_1'$, but allowing for its radial orientation, the mean net lateral friction can be shown to be
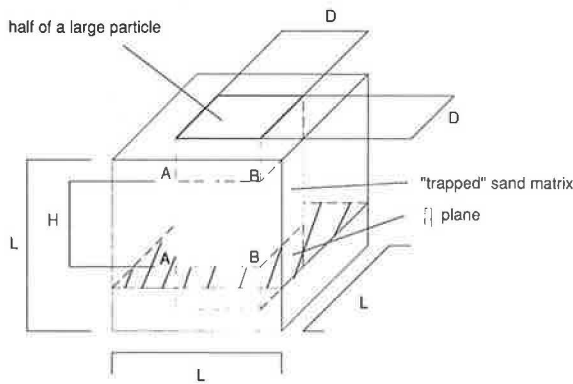
approximately $0.5 \mu\sigma_1'$. Then for equilibrium with a central lateral stress $\sigma_{3,c}$:

$$\sigma_{3,c}' \, H \cdot D = \sigma_3' \, H \cdot D + 0.5 \, \mu\sigma_1' \cdot D^2/2 \cdot 2$$

$$\therefore \sigma_{3,c} = \sigma_3' \, (1 + 0.5 \, \mu K_p \, D/H) \qquad (10)$$

The central axial stress is therefore

$$\sigma_{1,c}' - \sigma_3' \, K_p \, (1 + 0.5 \, \mu K_p \, D/H) \qquad (11)$$

Figure 12 shows the expected variation of axial stress across the whole unit cell. Allowing for the respective areas on which these stresses act, the mean axial stress is given by

$$\sigma_1' = K_p \cdot \sigma_3' + 0.5 \, \mu K_p^2 \, D/H \, \sigma_3' \cdot 1/2 \cdot A_R \qquad (12)$$

or substituting for A_R from Equation 7:

$$\frac{\sigma_1'}{\sigma_3'} = K_p \cdot [1 + (0.25 \, \mu \, K_p R)/(1 - R^{1/3})] \qquad (13)$$

where the failure stress-ratio is enhanced, due to the large particles, by the factor in the brackets. This should represent the largest possible enhancement of strength, because the particles have been given ideally flat surfaces, parallel to each other.

Substituting $K_p = 4$, $\mu = 0.5$, $R = 0.21$ (relevant to $P = 30$ percent large particles at $e = 0.4$), the enhancement factor in Equation 13 estimated to be 1.26. This would indicate a new value $\phi' = 42°$, with an enhancement $\Delta\phi' = 5°$. If this is about double the effect shown in Figure 8, it might be taken to represent a statistical discrepancy due to the irregular shape of the actual large particles and their disposition.

FIGURE 10   Unit cell for the strengthening effect.
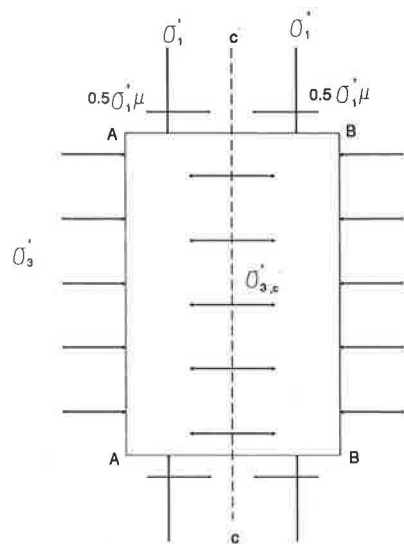
FIGURE 11   Equilibrium of unit cell across central cross section of matrix soil.

CONCLUSION

An investigation has been carried out into the effects on shear strength of soil including a proportion of large particles in an otherwise conventional sound fill. It was found that some
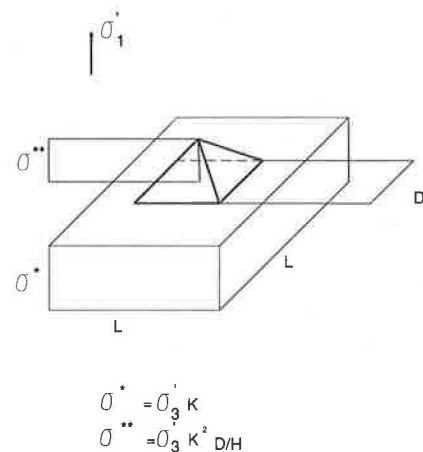

$$\sigma^* = \sigma_3' \, K$$
$$\sigma^{**} = \sigma_3' \, K^2 \, D/H$$

FIGURE 12   Distribution of major principal stress.

small variation occurred in the angle of shearing resistance (ϕ') when the various soils were compacted to target relative densities. A well-compacted mixture with 15 percent of large particles could lose 1.5° in ϕ', whereas with 30 percent of large particles a gain of about 3° was available. These effects were explained by reference on one hand to disturbance of packing in the vicinity of sparse inclusions, and on the other to an internal reinforcement of matrix soil trapped between large inclusions, analogous to that found in triaxial tests with rough platens.

Similar effects were found (at low stress levels appropriate to road embankments) irrespective of whether the large inclusions were as strong as the matrix, or were five times more friable. This raises the question of the potential use of inexpensive or waste materials at a proportion of 30 percent to a good fill, which might result in a composite backfill even stronger than that of the 100 percent high-quality fill. More work on field compaction, specification, and control would be necessary before such advantage could be realized in practice.

ACKNOWLEDGMENT

REFERENCES

1. *Specification of Highway Works.* Part 2. Department of Transport, Her Majesty's Stationery Office, London, United Kingdom, 1986.
2. M. D. Bolton. The Strength and Dilatancy of Sands. *Geotechnique 36*, No. 1, 1986, pp. 65–78.
3. A. J. Brown. Use of Soft Rockfill at Evretou Dam, Cyprus. *Geotechnique 38*, No. 3, 1988, pp. 333–354.
4. A. A. Griffith. The Phenomena of Rupture and Flow in Solid. Phil. Tran. Roy. Soc. (London) A221, 1920, pp. 163–198.
5. W. C. Krumbein. Measurement and Geologic Significance of Shape and Roundness of Sedimentary Particles. *Journal of Sedimentary Petrology*, Vol. 11, 1941, pp. 64–72.
6. G. Rittenhouse. A Visual Method of Estimating Two-Dimensional Sphericity. *Journal of Sedimentary Petrology*, Vol. 13, 1943, pp. 79–81.
7. A. W. Bishop and D. J. Henkel. *The Measurement of Soil Properties in the Triaxial Test.* Edward Arnold, 1957.
8. F. H. Siddiqi. *Strength Evaluation of Cohesionless Soils with Oversize Particles.* Ph.D. thesis. University of California, Davis, 1984.
9. N. D. Marachi, C. K. Chan, and H. B. Seed. Evaluation of Properties of Rockfill Materials. *J. SMFE Div.*, ASCE, Vol. 98: SMI, pp. 95–114.
10. M. Al-Hussaini. Effect of Particle Size and Strain Conditions on the Strength of Crushed Basalt. *Canadian Geotechnical Journal*, Vol. 20, 1983.
11. W. Su. *Static Strength Evaluation of Cohesionless Soil with Oversize Particles.* Ph.D. thesis. Washington State University, 1989.
12. G. T. Houlsby. *A Study of Plasticity Theories and Their Applicability to Soils.* Ph.D. thesis. University of Cambridge, Cambridge, England, 1981.
13. R. J. Fragaszy, W. Su, and F. H. Siddiqi. Effects of Oversize Particles on Density of Clean Granular Soils. *Geotechnical Testing Journal*, ASTM, Philadelphia, Pa. Vol. 12, No.2, pp. 106–114.